ВАК 2024 MODERN ASTRONOMY: FROM THE EARLY UNIVERSE TO EXOPLANETS AND BLACK HOLES
300 years Russian Academy of Sciences

Investigation of the dynamics of the magnetic field and vertical electric current during the precursors of the M6.5 class solar flare of June 22, 2015 using vector 135-second HMI magnetograms

I. Sharykin and I. Zimovets

Space Research Institute of Russian Academy of Sciences, Profsoyuznaya Str. 84/32, Moscow, 117485 Russia

Abstract. This paper considers the M6.5 eruptive solar flare occurred on June 22, 2015, for which ultraviolet preflare emission sources in the 1600 Å chromospheric channel have been analyzed using AIA/SDO data. Magnetic fields at the photospheric level are also analyzed using HMI/SDO vector magnetograms with a time resolution of 135 seconds. Since the selected flare has a long preflare phase (about one hour), the available time resolution of vector magnetograms is sufficient to study the flare and preflare dynamics of magnetic fields at the photospheric level. It can be noted that the literature mainly considers the change in currents during solar flares, while insufficient attention is paid to precursors. Our main goal is to provide continuous monitoring of the dynamics of electric current during the preflare period, at the beginning of the flare and during the main phases of the flare. We determined the magnetic flux (and its time derivative) in the preflare sources at the chromospheric level in comparison with the magnetic fluxes of the flare ribbons. Analysis of 135-second HMI photospheric vector magnetograms showed that there was an increase in the total vertical electric current about 1 hour before the flare. During this hour, there were variations of the mean vertical electric current density and its subsequent drop during the flare. We probably see an intermittent increase and dissipation of currents due to individual bursts in the preflare region. Also, the analysis of magnetic fluxes showed that, despite the weak preflare soft X-ray fluxes, the variations in magnetic flux during precursors are comparable in order of magnitude to what we see during the main phase of the solar flare. The difference between the time derivatives of the magnetic flux for precursor radiation sources and flare ribbons does not exceed a factor of 3.

Keywords: Sun: solar flares; precursors; magnetic field; electric current

DOI: 10.26119/VAK2024.114

1 Introduction

Precursor activity before solar flares is usually studied in the context of space weather forecasting. It is very important to understand the features of the energy accumulation processes in active regions that produce flares and coronal mass ejections. Usually precursors are considered as different transient emission brightnings or structures before the flares in the parent active region seen in different types of electromagnetic emission (e.g., Bamba et al. 2017). Despite our knowledge of the morphology of preflare processes, we do not have detailed information on the changes in the magnetic field during the preflare stage. We also have no information on the dynamics of reconnection of magnetic flux and electric currents in the time range from precursor processes to the onset of the flare, which turns into a developed impulsive phase. The main goal of the work is to capture the features of the electrodynamics of preflare processes in comparison with the subsequent impulsive phase. For this purpose, a flare (briefly described in the abstract, and also studied by the authors in the work of Artemyev et al. 2021) was selected with a well-defined grouping of precursors 1–2 hours before the flare. To study the magnetic field dynamics, we use the available high-cadence 135-second vector magnetograms (Sun et al. 2017) from HMI (Scherrer et al. 2012).

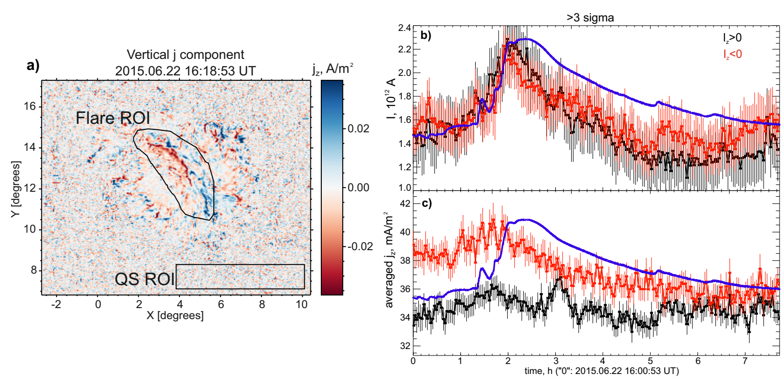

Fig. 1. Panel (a) shows the vertical electric current (j_z) map calculated from the 135-second HMI vector magnetograms. The flare ROI is marked by irregular black contour covering flare j_z "ribbons" of opposite polarities. The rectangular ROI corresponds to the place used for determination of the j_z distribution and estimation of the j_z error. Time profiles of total vertical electric current I_z and average value of j_z are shown in (b) and (c), respectively. The blue curve is the GOES X-ray lightcurve in the 1–8 Å channel.

2 Flare and preflare electrodynamics

Dynamics of the total vertical electric currents and the averaged current density in the flare region (ROI in panel a) is shown in Fig. 1 in the corresponding panels b and c. It can be noted that the gradual increase in the X-ray flux was associated with an increase in the total vertical current, amounting to only $j_z > 3\sigma$ (b). The precursory phase was accompanied by the variations of vertical current density (1–2 hours in panel (c)).

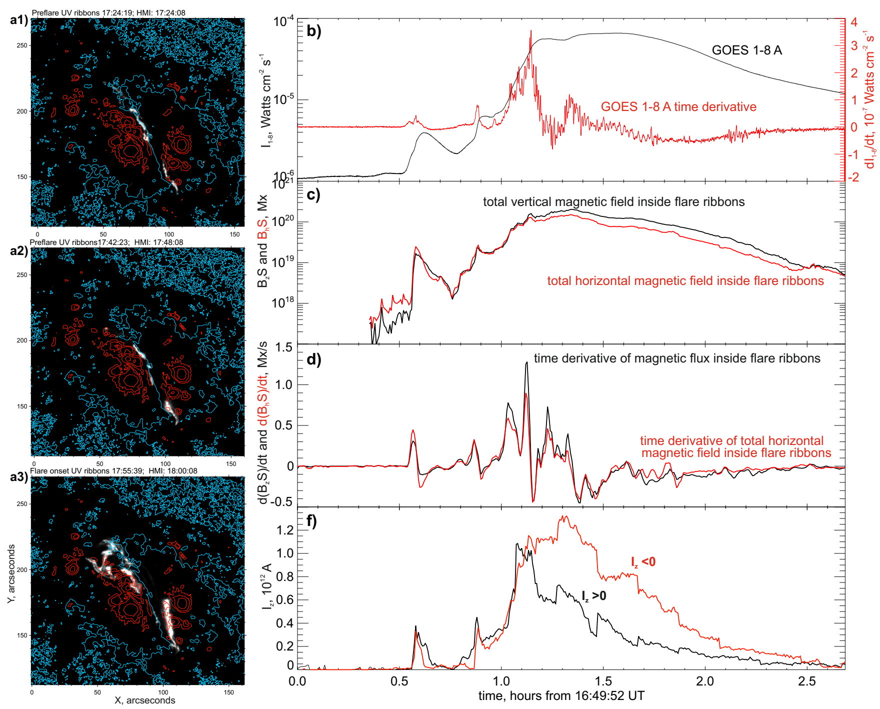

Fig. 2. Panels (a1–a3) show the preflare UV sources and the flare ribbon in the background layer compared with the superimposed B_z (red) and PIL (blue) contours. GOES X-ray 1–8 Å flux (black) and its time derivative (red) are shown in panel (b). Magnetic fluxes of vertical (black) and horizontal (red) magnetic field inside flare ribbons are shown in panel (c) and its time derivatives in panel (d). The dynamics of the total vertical electric current inside the flare ribbons is shown in (f): red and black colors correspond to negative and positive values of j_z.

We use chromospheric ultraviolet images to obtain regions of the energy release in the preflare and flare regions. The dynamics of the UV emission sources can be seen in Fig. 2(a1–a3). Initial preflare emission sources were located close to the PIL then flare ribbons began to move out of the PIL. For the regions above 300 DNs we calculated magnetic flux (Fig. 2(c)) and its time derivative (d) usually associated with the reconnecting magnetic flux (e.g., Sharykin et al. 2020). It can be seen that the initial preflare brightnings ($t = 0.4 - 0.6$ h) were mostly in the horizontal magnetic field and the reconnecting magnetic flux was approximately two orders less then the peak during the flare. It can be noted that the largest reconnected flux during the precursor phase around $t = 0.6$ h was only one order of magnitude smaller than the peak. The values of the reconnecting magnetic flux derivative during the precursor is only 2–3 times less than the peak rate. Moreover, the characteristic duration of the precursor reconnection rate is comparable to individual peaks during the flare.

3 Concluding remarks

Analysis of the HMI 135-second vector magnetograms with the dynamics of the preflare/flare chromospheric emission sources revealed variations of the electric current density during the precursors. We probably recorded signs of dissipation of electric currents around the twisted magnetic structure along the LIP, where the precursors were localized. An analysis of the dynamics of the magnetic field around the preflare and flare emission sources showed that the precursor can be considered as an "individual" pulse-like episode of energy release, while the entire flare process is an avalanche-like process of many similar episodes of energy release (pile-up of pulses) with reconnection rates and characteristic times comparable to the preflare ones. Localized emission sources in PILs with high reconnection rates in the active region can be considered as tracers of preflare accumulation. Perhaps this fact can be used to predict solar flares once more statistical information is available.

Acknowledgements. We thank the many team members who contributed to the success of the SDO mission and, especially, the HMI instrument.

Funding

The work was supported by the Russian Science Foundation grant No. 20-72-10158.

References

Artemyev A., Zimovets I.V., Sharykin I.N., 2021, Astrophysical Journal, 923, id. 151
Bamba Y., Lee K.-S., Imada S., Kusano K., 2017, Astrophysical Journal, 840, id. 116
Sharykin I.N., Zimovets I.V., Myshyakov I.I., 2020, Astrophysical Journal, 893, id. 159
Scherrer P.H., Schou J., Bush R.I., et al., 2012, Solar Physics, 275, p. 207
Sun X., Hoeksema J.T., Liu Y., et al., 2017, Astrophysical Journal, 839, id. 67